Influence of land-atmosphere feedbacks on temperature and precipitation extremes in the GLACE-CMIP5 ensemble

Ruth Lorenz[1], Daniel Argüeso[1], Markus G. Donat[1], Andrew J. Pitman[1], Bart van den Hurk[2], Alexis Berg[3], David M. Lawrence[4], Frédérique Chéruy[5], Agnès Ducharne[6], Stefan Hagemann[7], Arndt Meier[8], P. C. D. Milly[9], and Sonia I. Seneviratne[1,10]

[1] ARC Center of Excellence for Climate System Science and Climate Change Research Center, University of New South Wales, Sydney, New South Wales, Australia, [2] Royal Netherlands Meteorological Institute, De Bilt, Netherlands, [3] International Research Institute for Climate and Society, Earth Institute, Columbia University, Palisades, New York, USA, [4] National Center for Atmospheric Research, Boulder, Colorado, USA, [5] LMD/IPSL, Palaiseau, Paris, France, [6] UPMC, CNRS, EPHE, UMR 7619 Metis, Sorbonne Universités, Paris, France, [7] Max Planck Institute for Meteorology, Hamburg, Germany, [8] Centre for Environmental and Climate Research (CEC), Lund University, Lund, Sweden, [9] U. S. Geological Survey, Princeton, New Jersey, USA, [10] Institute for Atmospheric and Climate Science, ETH Zurich, Zurich, Switzerland

Abstract We examine how soil moisture variability and trends affect the simulation of temperature and precipitation extremes in six global climate models using the experimental protocol of the Global Land-Atmosphere Coupling Experiment of the Coupled Model Intercomparison Project, Phase 5 (GLACE-CMIP5). This protocol enables separate examinations of the influences of soil moisture variability and trends on the intensity, frequency, and duration of climate extremes by the end of the 21st century under a business-as-usual (Representative Concentration Pathway 8.5) emission scenario. Removing soil moisture variability significantly reduces temperature extremes over most continental surfaces, while wet precipitation extremes are enhanced in the tropics. Projected drying trends in soil moisture lead to increases in intensity, frequency, and duration of temperature extremes by the end of the 21st century. Wet precipitation extremes are decreased in the tropics with soil moisture trends in the simulations, while dry extremes are enhanced in some regions, in particular the Mediterranean and Australia. However, the ensemble results mask considerable differences in the soil moisture trends simulated by the six climate models. We find that the large differences between the models in soil moisture trends, which are related to an unknown combination of differences in atmospheric forcing (precipitation, net radiation), flux partitioning at the land surface, and how soil moisture is parameterized, imply considerable uncertainty in future changes in climate extremes.

1. Introduction

Extreme climate and weather events present major risks for ecosystems and society [*Seneviratne et al.*, 2012]. Observations show that characteristics of many extreme events, such as heat waves, occurrence of warm nights, and heavy rainfall events, are already changing [*Frich et al.*, 2002; *Alexander et al.*, 2006; *Seneviratne et al.*, 2012] with trends in hot temperature extremes being particularly robust [*Perkins et al.*, 2012; *Donat et al.*, 2013]. Many extremes are expected to change in the future under higher atmospheric CO_2 concentrations [*Easterling et al.*, 2000; *Frei et al.*, 2006; *Orlowsky and Seneviratne*, 2011; *Seneviratne et al.*, 2012; *Sillmann et al.*, 2013]. While internal climate variability (on decadal, interannual, and subseasonal timescales) leads to large uncertainties at local and regional scales [*Fischer et al.*, 2013; *Fischer and Knutti*, 2014], at global scales climate models generally agree on the forced response pattern for temperature and precipitation extremes [*Fischer et al.*, 2014; *Fischer and Knutti*, 2014].

Land surface processes influence the boundary layer and the atmosphere and affect extreme events [*Seneviratne et al.*, 2010; *Pitman et al.*, 2012]. Several recent investigations into the effect of land-atmosphere feedbacks on extremes have focused on analyses of observations. For example, *Hirschi et al.* [2010] identify an impact of soil moisture on hot extremes in southeastern Europe and relate this impact to the prevailing climate regime in that region (soil moisture-limited evapotranspiration regime). Wet conditions inhibit hot

summer days, whereas during dry conditions a larger number of hot summer days is more likely. *Quesada et al.* [2012] generalize this result for all of Europe, and *Ford and Quiring* [2014] find similar results for Oklahoma (U.S.). *Mueller and Seneviratne* [2012] present a global observational study indicating that a large fraction of the globe displays an increase in the probability of hot extremes following surface moisture deficits.

A larger amount of work has examined land-atmosphere interactions and their impacts on climate variability and extremes using climate models. *Seneviratne et al.* [2006] investigate the impacts of soil moisture-climate interactions for projected changes in interannual summer climate variability in Europe, identifying that about 60% of the variability can be related to these feedbacks in transitional climate regimes. *Fischer et al.* [2007] show that interactions between soil moisture and temperature can increase heat wave duration in Europe and account for 50–80% of hot summer days in this region. *Jaeger and Seneviratne* [2011] show that intraseasonal and interannual variability in soil moisture accounts for 5–30% and 10–40% of heat wave anomalies in Europe, respectively. *Vautard et al.* [2007], *Haarsma et al.* [2009], and *Zampieri et al.* [2009] also identify nonlocal mechanisms relating dry soils and hot extremes, finding that dry soils in southern Europe enhance the northward spread of heat and dryness. In the U.S., previous studies suggest that drought conditions induce warming in central parts of the continent [*Durre et al.*, 2000; *Donat et al.*, 2015] and that this effect is larger when the Pacific Ocean is in a cold phase [*Koster et al.*, 2009]. Finally, a study for Australia identifies that soil moisture-temperature feedbacks are most relevant for daily maximum temperatures in that region [*Hirsch et al.*, 2014]. The impact of soil moisture on precipitation is more uncertain due to the presence of both direct and indirect effects [e.g., *Eltahir and Bras*, 1996; *Ek and Holtslag*, 2004; *Taylor et al.*, 2011; *Guillod et al.*, 2015]. Direct effects are based on moisture recycling within a region, while the indirect effects include several aspects, e.g., impacts on the planetary boundary layer, modifications of (mesoscale) circulation patterns, and influences from soil moisture states outside the affected region [e.g., *Schär et al.*, 1999; *Seneviratne et al.*, 2010; *Taylor et al.*, 2011; *Goessling and Reick*, 2011]. *Douville* [2002] find soil moisture relaxation to be beneficial for simulating the variability in Sahelian monsoon rainfall, while it has no effect on the Asian monsoon. In a study over South America, *Sörensson and Menéndez* [2011] find evapotranspiration recycling to be important in the La Plata Basin and North East Brazil enhancing extreme precipitation events in the former region. However, they also find that the feedback between soil moisture and the occurrence of heavy precipitation may be negative or positive depending on the region. Finally, *Jaeger and Seneviratne* [2011] find small impacts from soil moisture variability on the frequency of wet precipitation extremes in Europe, but *Diro et al.* [2014] find that land surface processes may have an influence on the persistence of high precipitation days in western North America.

Here we present a detailed multimodel analysis of the impact of soil moisture-climate interactions on temperature and precipitation extremes in the present and in the future. We use the experimental protocol of the Global Land-Atmosphere Coupling Experiment of the Coupled Model Intercomparison Project, Phase 5 (GLACE-CMIP5) [*Seneviratne et al.*, 2013]. This protocol applies prescribed soil moisture experiments over the period 1950–2100 to investigate how changes in soil moisture content and variability affect extremes. We build on three earlier analyses. First, *Seneviratne et al.* [2013, hereafter S13] used the GLACE-CMIP5 experimental database to show that projected changes in soil moisture affect summer temperature, in particular extreme temperature, and mean and extreme precipitation (although less consistently). S13 considered impacts of soil moisture-climate interactions on the 95th percentile of temperature in projections but did not consider a wider range of indices or impacts in the present climate. Second, *Berg et al.* [2014] used the GLACE-CMIP5 experimental database to analyze the influence of soil moisture dynamics on temperature distributions in the historical period using the Geophysical Fluid Dynamics Laboratory (GFDL) model and find an asymmetric impact on the positive and negative extremes of the temperature distributions. *Berg et al.* [2015] analyzed the correlation of seasonal temperature and precipitation in the same models and experiments as S13 and found that long-term regional warming is modulated by the projected trends in precipitation. Finally, *May et al.* [2015] related the projected climate changes in the tropics to the projected changes in soil moisture and found that about 80% of the change in energy fluxes and temperature can be related to soil moisture changes, whereas only 30–40% of precipitation change can be so related. They also report that even though there are regional differences in the projected climate changes between the models, the basic mechanisms of soil moisture-temperature and soil moisture-precipitation coupling work similarly in the different GLACE-CMIP5 models.

We analyze three modeling experiments from the GLACE-CMIP5 protocol (see also S13): the control (CTL) simulation with fully interactive soil moisture, experiment 1A (here referred to as SMclim), in which the

seasonal cycle of soil moisture is prescribed to the CTL climatology from 1971 to 2000, and the experiment 1B (here referred to as SMtrend), in which soil moisture is prescribed to a transient seasonal CTL climatology (see section 2.1 for more details). These experiments provide a unique opportunity to examine the influence of soil moisture on extremes within a model ensemble. Using models that participated in CMIP5, a cause-and-effect analysis can then be attempted at the global scale in transient climate simulations.

2. Methods

2.1. Overview of Experiments

GLACE-CMIP5 provides model simulations for the period 1950–2100 from six global climate models: Australian Community Climate and Earth System Simulator (ACCESS), Community Earth System Model (CESM), EC-EARTH, European Centre/Hamburg Model 6 (ECHAM6), GFDL Model, and Institut Pierre-Simon Laplace Model. The two perturbed experiments are atmosphere/land only with prescribed sea surface temperatures (SSTs) and sea ice distribution. As first reported by S13 (see their Table 1) the configuration of the control simulations (CTL) varied among models, with some simply using a fully coupled CMIP5 simulation and some using a new Atmospheric Model Intercomparison Project (AMIP)-style [*Gates*, 1992] control simulation, utilizing SSTs and sea ice from the same models CMIP5 coupled simulation. ECHAM6 later contributed an AMIP-style CTL simulation, which we used in this study. We note that some minor differences in model configurations exist relative to the published CMIP5 models. In all experiments, the SSTs, sea ice distribution, and atmospheric carbon dioxide (CO_2) concentrations (RCP8.5) [*Meinshausen et al.*, 2011] from the CMIP5 simulations were used for the period 2006–2100.

In the first experiment, SMclim (1A in S13), the soil moisture mean annual cycle averaged for 1971–2000 is prescribed using soil moisture from each model's control simulation. The second experiment, SMtrend (1B in S13), is identical except that a transient climatology is used to prescribe soil moisture. Specifically, the seasonal cycle of soil moisture for the years 1980–2070 is prescribed using the 30 year running mean from the control run, and the first and last 15 years of each experiment use the climatology of 1950–1979 and 2071–2100, respectively. Depending on the model, soil moisture of the whole soil column was prescribed every time step, daily, or monthly with interpolation between the midpoints of the adjacent months for each time step. This paper adds the Australian Community Climate and Earth System Simulator (ACCESS) model [*Bi et al.*, 2013] to the ensemble, which was also a contributor to CMIP5. We used ACCESS1.3b and undertook a new control simulation because the land surface model (Community Atmosphere Biosphere Land Exchange) [*Kowalczyk et al.*, 2013] had been updated (see *Lorenz et al.* [2014] for more details). In ACCESS, SSTs and sea ice distribution based on AMIP were used for the historical period (1951–2006), and CMIP5 input data were used for the period 2007–2100 (whereas in the other models, CMIP5 input data were used throughout). Where the change in SSTs from historical to future period in ACCESS matters, we exclude ACCESS from the analysis.

2.2. Extreme Indices

We calculate indices that measure the intensity, frequency, and duration of extreme climate events as recommended by the Expert Team on Climate Change Detection and Indices (ETCCDI) plus an additional heat wave index. The ETCCDI indices are calculated from daily maximum (T_{max}) and minimum temperature (T_{min}) and daily precipitation (http://www.climdex.org/indices.html). Most of these indices describe relatively moderate extremes with return periods of a year or shorter. We calculate all indices using freely available software (http://www.climdex.org/climdex_software.html) but present only a subset here (Table 1). The intensity of hot extremes is represented by the warmest daily maximum temperature each year (hottest day, TXx), while the frequency is expressed by the percentage of days per year when the daily maximum temperature exceeds the 90th percentile calculated for the 1961–1990 base period (warm days, TX90p). The default software was modified to enable the use of percentiles calculated from 1961 to 1990 in the control simulation for the two experiments. The duration of extreme temperature conditions is measured with the Heat Wave Duration (HWD) index based on, e.g., *Perkins and Alexander* [2013]. This index is based on daily temperatures and is the longest period of three or more consecutive days when the 3 day average of the daily average temperature is greater than the 90th percentile (T90). T90 is calculated for each calendar day using a 15 day window for the 1961–1990 period. We use the historical 90th percentile calculated for the 1961–1990 base period from the CTL to ensure consistency with TX90p. This means that we compare future temperatures to the same extreme threshold as historical temperatures. To evaluate how the impact of heat waves on human health or comfort may change over a climate period, one has to make assumptions on adaptation of humans. By using the historical 90th percentile we implicitly assume that this human adaptation to future conditions is absent.

Table 1. Extreme Indices Used in This Study[a]

Index	Indicator Name	Definition	Unit
Temperature			
Intensity			
TXx	max T_{max}	Warmest daily maximum temperature	°C
Frequency			
TX90p	Warm days	Percentage of time when daily max temperature >90th percentile	%
Duration			
HWD	Heat wave duration	Duration of the longest heat wave per year where 3 day daily average temperature exceeds 90th percentile for at least three consecutive days, 90th percentile calculated for each calendar day using a 15 day window	days
Precipitation			
Intensity			
R95p	Contribution from very wet days	Annual sum of daily precipitation $\geq$ 95th percentile	mm
Frequency			
R10mm	Heavy precipitation days	Number of days when precipitation $\geq$ 10 mm	days
Duration			
CDD	Consecutive dry days	Maximum number of consecutive days when precipitation < 1 mm	days
CWD	Consecutive wet days	Maximum number of consecutive days when precipitation > 1 mm	days

[a]Percentiles are calculated over base period 1961–1990. SMclim and SMtrend are compared to percentile calculated from CTL for temperature indices.

For precipitation we analyze annual sums of daily precipitation above the 95th percentile (contribution from very wet days, R95p) for intensity, the number of days when precipitation is larger than 10 mm (heavy precipitation days, R10mm) for the frequency, and the maximum number of consecutive days above and below 1 mm (consecutive wet days, CWD, and consecutive dry days, CDD, respectively) for the duration of the longest wet and dry spells in a year.

We focus on the differences between CTL and SMclim in the historical period (1971–2000) and SMclim and SMtrend in the second half of this century (2056–2085). Due to the missing trend in the last 15 years of SMtrend, caused by the unavailability of data for the 30 year running mean, we only analyze data until 2085. Note that this latter time period is different from that considered in S13 (2071–2100), although this does not strongly affect the results (not shown).

The ensemble mean differences were calculated as the mean of each individual model's difference to avoid influences from model biases. The indices were calculated for each model on its native grid and then regridded to a common grid defined by the lowest resolution of the participating climate models (1.895° latitude by 3.75° longitude). We used the Climate Data Operators conservative remapping for the interpolation. The signals were tested for statistical significance on a 5% level using a Kolmogorov-Smirnov test (KS test) on the local 30 year ensemble mean time series at each grid cell.

2.3. Spatially Aggregated pdfs

For a regional analysis (defined by the boxes in Figures 1a and 2a) we used spatially aggregated probability density functions (pdfs) following *Fischer and Knutti* [2014]. The data were weighted by the latitude-dependent area, and we omitted grid points that were not identified as land by more than half of the
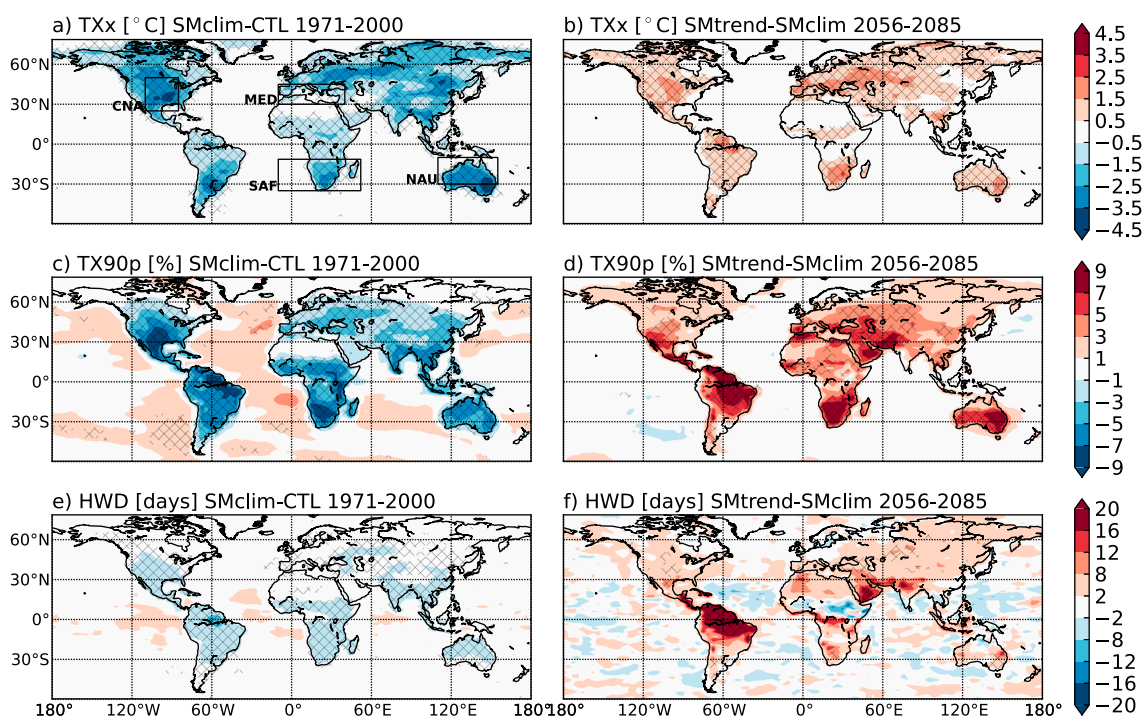
Figure 1. (a and b) Warmest daily maximum temperature (intensity), (c and d) warm days (frequency), and (e and f) heat wave duration (duration). Multimodel mean, hatching where statistically significant (KS test, *p* value<0.05). Figures 1a, 1c, and 1e for SMclim-CTL in 1971–2000. Figures 1b, 1d, and 1f for SMtrend-SMclim in 2056–2085.

climate models. These regions, Central North America (CNA), the Mediterranean (MED), Southern Africa (SAF), Northern Australia (NAU), North East Brazil (NEB), East Africa (EAF), and South Asia (SAS), which are based on the definition of the Intergovernmental Panel on Climate Change (IPCC) Special Report on Extremes Regions [*Seneviratne et al.*, 2012], were chosen because these are likely regions of strong land-climate coupling [e.g., *Koster et al.*, 2006; *Miralles et al.*, 2012; *Seneviratne et al.*, 2013; *Lorenz et al.*, 2015]. The indices TXx, R10mm, CWD, and CDD are absolute quantities and not normalized by percentiles from CTL. Instead, they are normalized by removing the mean of the respective CTL of each climate model before calculating the pdfs to minimize the impact of model biases.

3. Results

3.1. Historical Period 1971–2000: SMclim Versus CTL

First, we compare SMclim to CTL in the historical period. This comparison examines the impact of removing interannual soil moisture variability, as well as most day-to-day variability, on our chosen extremes indices. Because SMclim and SMtrend are very similar during this time period, and none of the models exhibits a strong trend in soil moisture in the historical period, the comparison of SMtrend-CTL in this time period is almost identical. The 30 year average in the hottest day (TXx, Figure 1a) is significantly decreased in SMclim compared to CTL over almost all continental surfaces. The largest changes occur in Central North America, southern South America, South Africa, eastern China, Southeast Asia, and Australia, where reductions commonly exceed 1.5°C and reach 3.5°C over parts of North America and Australia. Similarly, numbers of warm days (TX90p, Figure 1c) are decreased over widespread regions. The reduction in TX90p is the largest in Central North America, northeastern Amazonia, and South Africa and in some regions exceeds 7% of days. The duration index HWD is generally decreased when interannual variability in soil moisture is removed (Figure 1e) by up to a week in many regions. The largest changes occur in Central North America, Amazonia, and Southern and Eastern Africa and reach about 5 days.

As expected, the results are less homogeneous for precipitation extremes, for which we find increases as well as decreases depending on the region. However, the regions where heavy precipitation is increased when soil moisture variability is removed are larger than the regions of decrease. The intensity of very wet days is
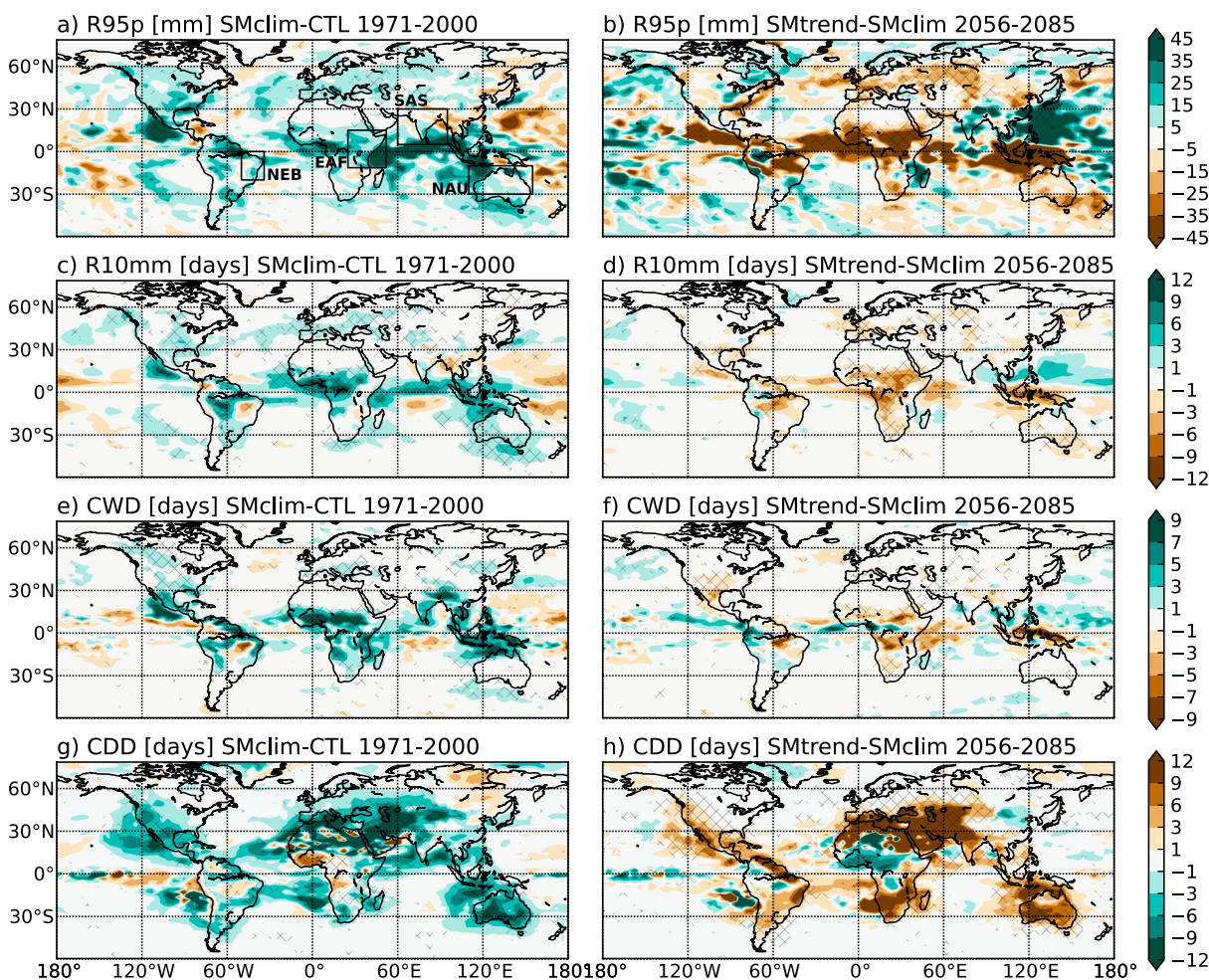
Figure 2. As Figure 1 but for annual contribution from (a and b) very wet days (intensity), (c and d) heavy precipitation days (frequency), (e and f) consecutive wet days (duration), and (g and h) consecutive dry days (duration).

increased in SMclim in particular in the tropics (Figure 2a). The frequency of days with precipitation larger than 10 mm is also increased in similar regions if soil moisture variability is removed (Figure 2c). The effect is largest in the tropics, where this increase exceeds 6 days, whereas it is rather small (1–3 days) or nonexistent outside of the tropics. A similar picture is found for the duration of precipitation events shown by the consecutive wet days (Figure 2e) which are increased up to 7 days and more in the Sahel and the Maritime continent. This increase is smaller, 1–5 days, in North America, the Mediterranean, India, South Africa, and the northern part of South America. The number of consecutive dry days (note that the color bar is inverted for Figure 2g) is mostly decreased. This effect is strongest in the Mediterranean and Middle East and also quite strong in Australia. In contrast, some areas of tropical West Africa show an increase in CDD when soil moisture variability is removed. Note that because CDD and CWD are the longest spells per year, both can increase in the same region.

3.2. Future Period 2056–2085: SMtrend Versus SMclim

The difference between SMtrend and SMclim in the second half of this century shows the influence of the long-term change in soil moisture by comparing the response of extreme indices to future and present day soil moisture climatological conditions. Consequently, areas in which soil moisture trends are absent will lead to indistinguishable results between SMclim and SMtrend. The intensity of hot days (TXx, Figure 1b) is higher in SMtrend than in SMclim, and the increase is statistically significant (p value<0.05) over large regions. The clearest signal (around 2.5°C) occurs in the central United States, Amazonia, Mediterranean, southeastern Europe, South Africa, Southeast Asia, and southeastern Australia. There is no difference in the Sahara, tropical Africa and parts of Asia. TX90p also is larger in SMtrend (Figure 1d), but the area of statistically significant differences is smaller in comparison to TXx, with some boreal regions of North America and Eurasia not
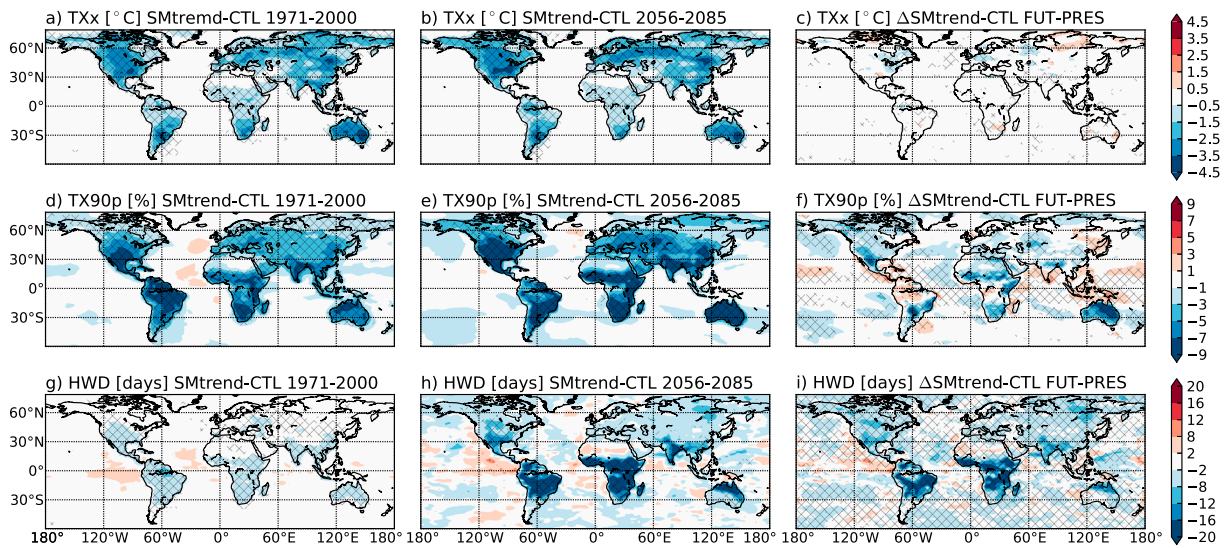
Figure 3. (a–c) Warmest daily maximum temperature (intensity), (d–f) warm days (frequency), and (g–i) heat wave duration (duration). Multimodel mean, hatching where statistically significant (KS test p value<0.05). Figures 3a, 3d, and 3g for SMtrend−CTL in 1971–2000; Figures 3b, 3e, and 3h for SMtrend−CTL in 2056–2085; and Figures 3c, 3f, and 3i the differences between 2056 and 2086 minus 1971 and 2000 in SMtrend-CTL (ACCESS excluded because of inconsistency in SSTs between two time periods, but this has almost no effect).

showing statistically significant changes. The regions with the most pronounced differences include Central North America, Central America, Amazonia, the Mediterranean, the Middle East, South Africa, and Australia. In general, the maximum duration of heat waves is also longer in SMtrend (Figure 1f), particularly in Amazonia where increases in HWD exceed 16 days. However, the regions with a statistically different signal in HWD are further decreased compared to those for TX90p but largely correspond to subsets of the regions where the differences in TX90p are statistically significant. The exceptions are tropical Africa, South East Asia, and North Australia where HWD is decreased in SMtrend. These results are consistent with S13's analyses of the changes in the mean temperature, daily T_{max}, and 95th percentile of T_{max}.

Again, the picture is more heterogeneous for precipitation extremes, but over land the regions where wet precipitation extremes are decreased with soil moisture trends predominate (Figures 2b, 2d, and 2f). For R95p this reduction is most pronounced in the tropics (Figure 2b), where it decreases by more than 35 mm. From Central to Eastern Europe and extending into North Asia we also find a significant decrease in R95p by up to 25 mm. Southeastern Australia also shows a decrease in R95p by similar amounts as in Europe. The regional pattern is similar in R10mm (Figure 2d), which shows decreases up to about 7 days in the tropics. In the extratropics the significant decreases are only between 1 and 3 days. Consecutive wet days are also mostly decreased in SMtrend but show a band of increase around the equator (Figure 2f). For instance, in Africa, CWD decrease south of the equator, while they increase just north of the equator and then decrease again further north in the Sahel. Dry periods, CDD (Figure 2h, note that the color bar is inverted), are increased in the Mediterranean and Middle East, North India, Australia, western U.S., Central America, north Amazonia, eastern and southern South America, and South Africa by more than 1 week. Some regions show a decrease in CDD, mainly in tropical Africa and bits of Amazonia.

3.3. Change in Influence From Soil Moisture Variability From Present to Future: SMtrend Versus CTL

Figure 3 shows the difference between SMtrend and CTL in 1971–2000 (Figures 3a, 3d, and 3g), 2056–2085 (Figures 3b, 3e, and 3h), and the difference between future and present (Figures 3c, 3f, and 3i) for temperature extremes. This analysis quantifies the influence of soil moisture variability on the change of temperature extremes with increased radiative forcing. Present and future values of TXx (Figures 3a and 3b) are hardly distinguishable, and their difference is below 1°C (Figure 3c shows Figure 3b minus Figure 3a). Hence, the influence of soil moisture variability on the intensity of temperature extremes remains similar under climate change. For TX90p we find that the difference between SMtrend and CTL is larger in the future (Figure 3e) than in the present period (Figure 3d) in several regions, namely, North America, South America outside Amazonia, Mediterranean, Sahel, East and South Africa, North India, and Australia (Figure 3f). However, the influence of soil moisture variability on TX90p is slightly smaller in the future in most of the tropics and North East China.
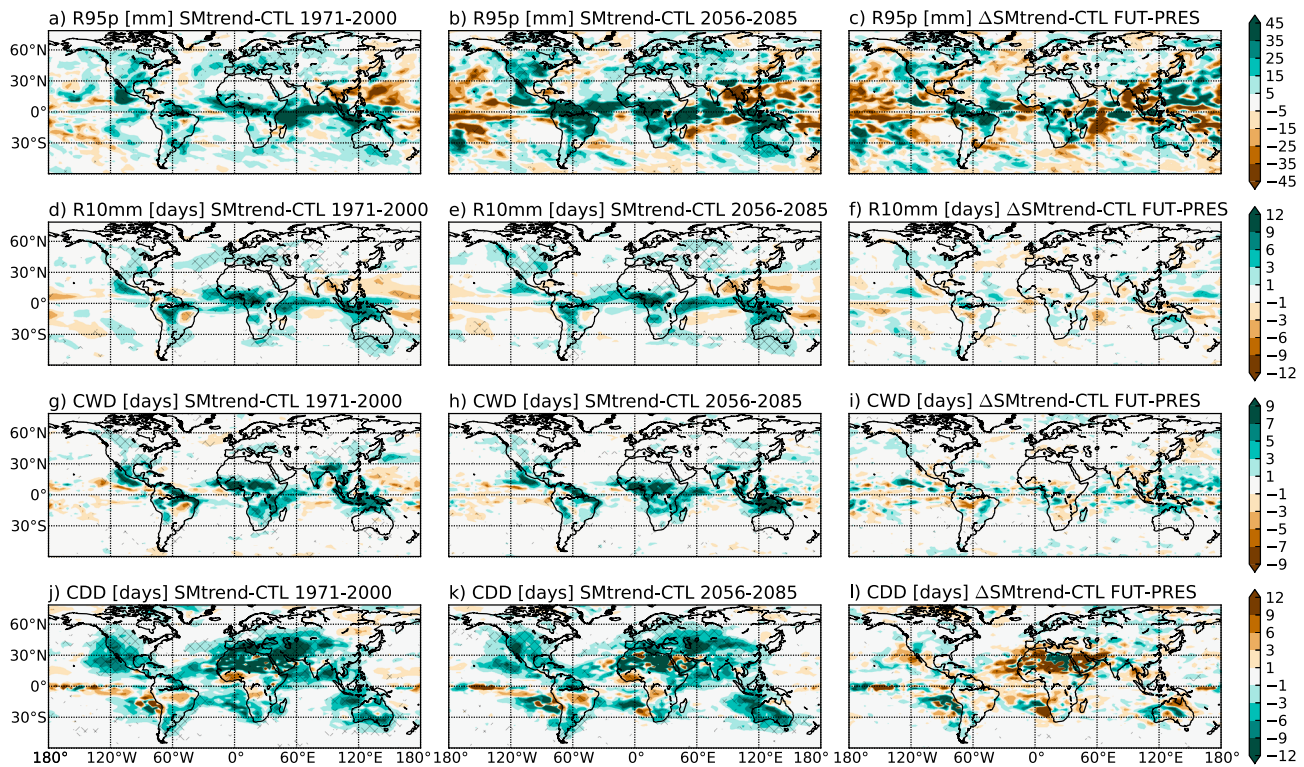
Figure 4. As Figure 3 but for annual contribution from (a–c) very wet days (intensity), (d–f) heavy precipitation days (frequency), (g–i) consecutive wet days (duration), and (j–l) consecutive dry days (duration).

For heat wave duration the difference between SMtrend and CTL is 2–8 days in the present (Figure 3g), while it can exceed 2 weeks in the future (Figure 3h). So the influence of soil moisture variability on heat wave duration is increased in the future in most areas, particularly in the wet tropics (Figure 3i).

For the precipitation extremes (Figure 4), the influence of soil moisture variability is rather similar under present and future conditions, and there are few regions with statistically significant differences (Figures 4c, 4f, 4i, and 4l). However, for R95p we do find an increased influence of soil moisture variability in Amazonia and tropical Africa and increased areas with statistically significant differences between SMtrend and CTL in the future (Figure 4b).

3.4. Future 2056–2085: Spatially Aggregated pdfs

Figure 5 shows the spatially aggregated pdfs for all temperature indices over four regions (see Figure 1a): Central North America (CNA), Mediterranean (MED), South Africa (SAF), and northern Australia (NAU). These regions are expected to be strongly influenced by soil moisture-atmosphere feedbacks [e.g., *Koster et al.*, 2006; *Miralles et al.*, 2012]. There is considerable variability in the shape and location of individual model results for TXx, TX90p, and HWD (thin lines). However, if aggregated over all models, the pdfs show that removing the interannual variability (SMclim and SMtrend) results in a clear shift toward lower values compared to CTL, a result that represents less intense, less frequent, and shorter hot extremes. For the hottest day (TXx, Figures 5a, 5d, 5g, and 5j) SMclim is the furthest to the left, in particular for CNA and MED, which suggests that interannual soil moisture variability plays an important role in defining very extreme temperatures in these regions. The multimodel aggregated pdfs for SMclim and SMtrend for TXx in NAU are similar. Because we subtract the local mean TXx of CTL of each model before calculating the TXx pdfs (to reduce the influence from model biases), negative values on the *x* axis correspond to values that are smaller than the long-term mean from CTL. For warm days TX90p, SMclim and SMtrend are also shifted to less frequent warm days, although this is less pronounced than for TXx. The multimodel aggregated pdfs for HWD are more similar to each other than for the intensity and frequency indices, indicating less influence from soil moisture variability and trend for this index. Nevertheless, the pdfs for SMclim and SMtrend peak for shorter heat waves than the CTL, and the CTL pdfs have a higher density for very long heat waves.
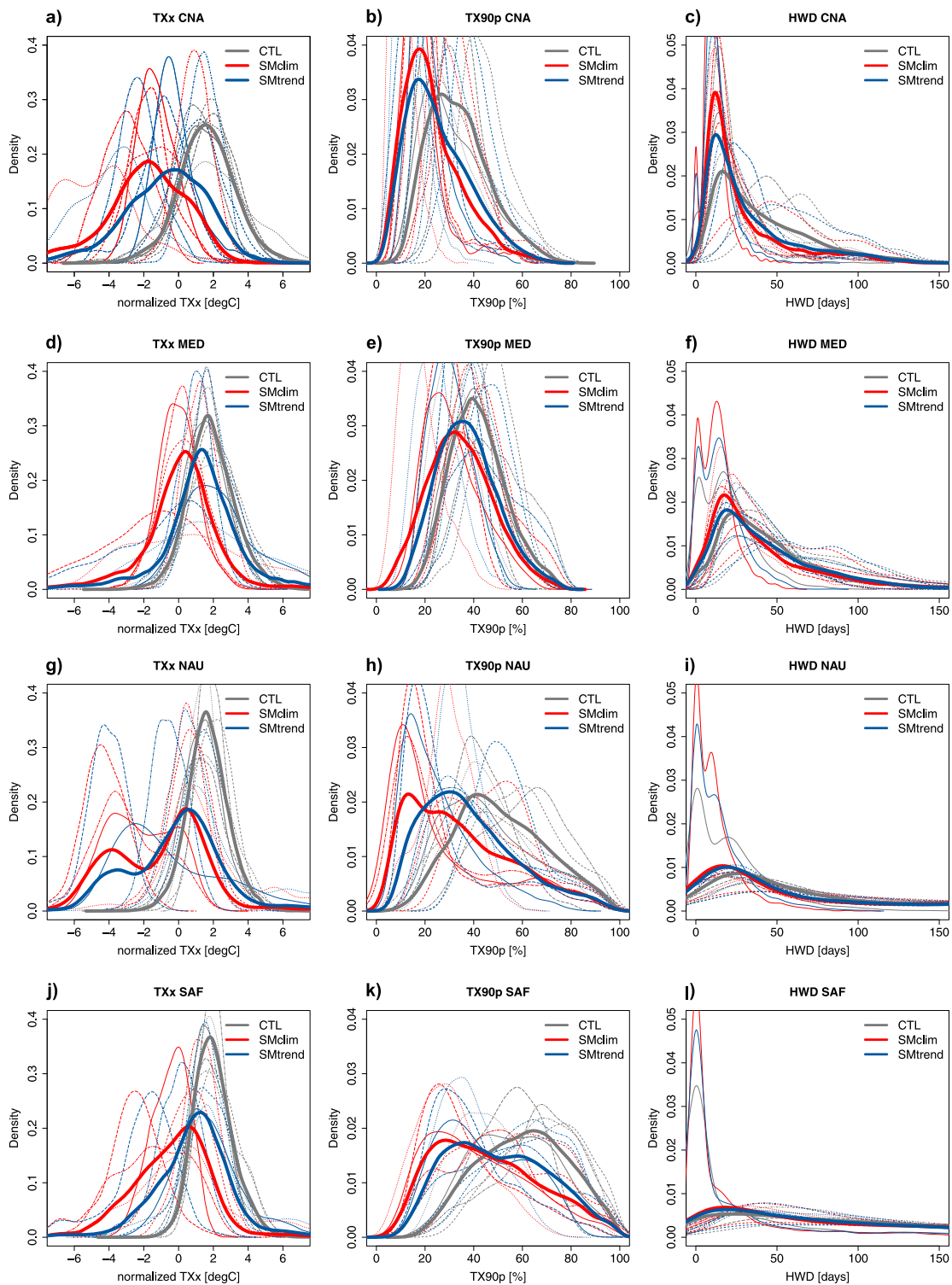
Figure 5. Spatially aggregated pdfs for temperature indices in the second half of the 21st century (2056–2085). The thin lines indicate the individual models, and the thick lines are the aggregated multimodel pdfs. TXx was normalized by removing the mean from each model's CTL. The regions are (a–c) Central North America (CNA), (d–f) Mediterranean (MED), (g–i) North Australia (NAU), and (j–l) South Africa (SAF).

For the precipitation indices we focus on different regions in comparison with temperature, these are North East Brazil (NEB), East Africa (EAF), South Asia (SAS), and North Australia (NAU). Despite selecting regions that are more suitable for examining differences in precipitation, the differences between the pdfs are small. For R95p (Figures 6a, 6e, 6i, and 6m) we see a slight shift to the right, towards more intense precipitation extremes, in NEB, EAF, and NAU, but SMclim and SMtrend only appear different for EAF and NAU. For R10mm we also find a slight shift to the right in NEB, EAF, and NAU (Figures 6b, 6f, 6j, and 6n). CWD NEB, EAF, and SAS show a slight shift to the right (Figures 6c, 6g, 6k, and 6o). The largest effects concern CDD, with pdfs for SMclim and SMtrend shifted to the left in all regions, in particular for SMclim (Figures 6d, 6h, 6l, and 6p). Even though these differences are small, they are statistically significant based on a 5% Kolmogorov-Smirnov test (*p* levels indicated by numbers in the graphs) except for R95p SMclim versus SMtrend in SAF.

4. Discussion

4.1. Effects From Removing Soil Moisture Variability and Trend

For the historical period 1971–2000, by definition the mean soil moisture climatology is the same in CTL and SMclim. Hence, the effects seen in Figures 1a, 1c, 1e, 2a, 2c, and 2e are almost solely caused by the removal of variability in soil moisture in SMclim. Only one model, CESM, used their fully coupled CMIP5 contribution as CTL where SST and sea ice can react to changing fluxes, which can cause additional differences. The intensity of hot extremes (TXx) is decreased by 0.5–4.5°C over all land areas except where the soil moisture is initially very dry (Figure 1a). The frequency of hot extremes (TX90p) is generally also decreased, commonly by 3–9% of days per year, with the exception of very dry areas and the very high latitudes that are not impacted (Figure 1c). The duration of heat waves (HWD) is also decreased in most areas, by 2–8 days, excluding some very dry areas (Sahara and Middle East) and the very high latitudes (Figure 1e). While the influence of soil moisture variability on regional hot extremes in the present climate has been shown in earlier modeling studies for Europe [e.g., *Seneviratne et al.*, 2006; *Fischer et al.*, 2007; *Jaeger and Seneviratne*, 2011; *Lorenz et al.*, 2013] and North America [*Koster et al.*, 2009; *Diro et al.*, 2014], this is the first demonstration of a systematic and widespread impact at the global scale in a multimodeling framework. Evidence to support this impact is provided by observationally based inferences using precipitation deficits as a proxy for soil moisture by *Mueller and Seneviratne* [2012]; these also suggested a widespread effect of soil moisture-temperature feedbacks for hot extremes. Soil moisture affects temperature by influencing the partitioning of latent and sensible heat flux, where drier soils generally lead to higher temperatures [e.g., *Seneviratne et al.*, 2010; *Yin et al.*, 2014]. Soil moisture also represents a memory component, similar to other slowly varying variables in the earth system such as land-ice, permafrost, or ocean temperatures. The decrease in extreme temperature indices caused by removing soil moisture variability suggests a dampening effect of soil moisture memory for temperature extremes at the global scale.

For precipitation, the results are more regionally heterogeneous. Wet precipitation extremes are more strongly influenced by soil moisture variability in the tropics, whereas dry extremes are more strongly influenced in the extra tropics. This is consistent with *Jaeger and Seneviratne* [2011] who found almost no effect from prescribed soil moisture on heavy precipitation in Europe. In GLACE-CMIP5, the removal of soil moisture variability increases the latent heat flux in soil moisture-limited regions (not shown but identified by *Berg et al.* [2014] for GFDL model) which tends to increase precipitation. To our knowledge, no previous study has investigated the influence of soil moisture variability on extreme precipitation in the tropics. For mean precipitation, negative and positive feedback loops are suggested in the literature [see, e.g., *Seneviratne et al.*, 2010]. Recently, *Guillod et al.* [2015] showed that afternoon precipitation tends to occur during wet and heterogeneous soil moisture conditions, located over comparatively drier patches. *Taylor et al.* [2013] found that regional climate models with parameterized convection schemes did not resolve the observed negative feedback between soil moisture and convective precipitation in the Sahel. The coarse resolution of our global climate models (GCMs) will lead to more homogeneous soil moisture patterns compared to observations, and we do not expect them to resolve possible negative soil moisture-precipitation feedbacks. Therefore, the reported positive soil moisture-precipitation feedback, i.e., the increase in wet precipitation extremes in SMclim compared to CTL, in the tropics in this study and also in *May et al.* [2015] might be influenced by the inability of the models to simulate the negative soil moisture-precipitation feedbacks. *Williams et al.* [2012] analyzed atmosphere-land feedbacks in some CMIP5 models — unfortunately those used in this study were not included — and their results highlight problems in the capability of the models to simulate a positive soil
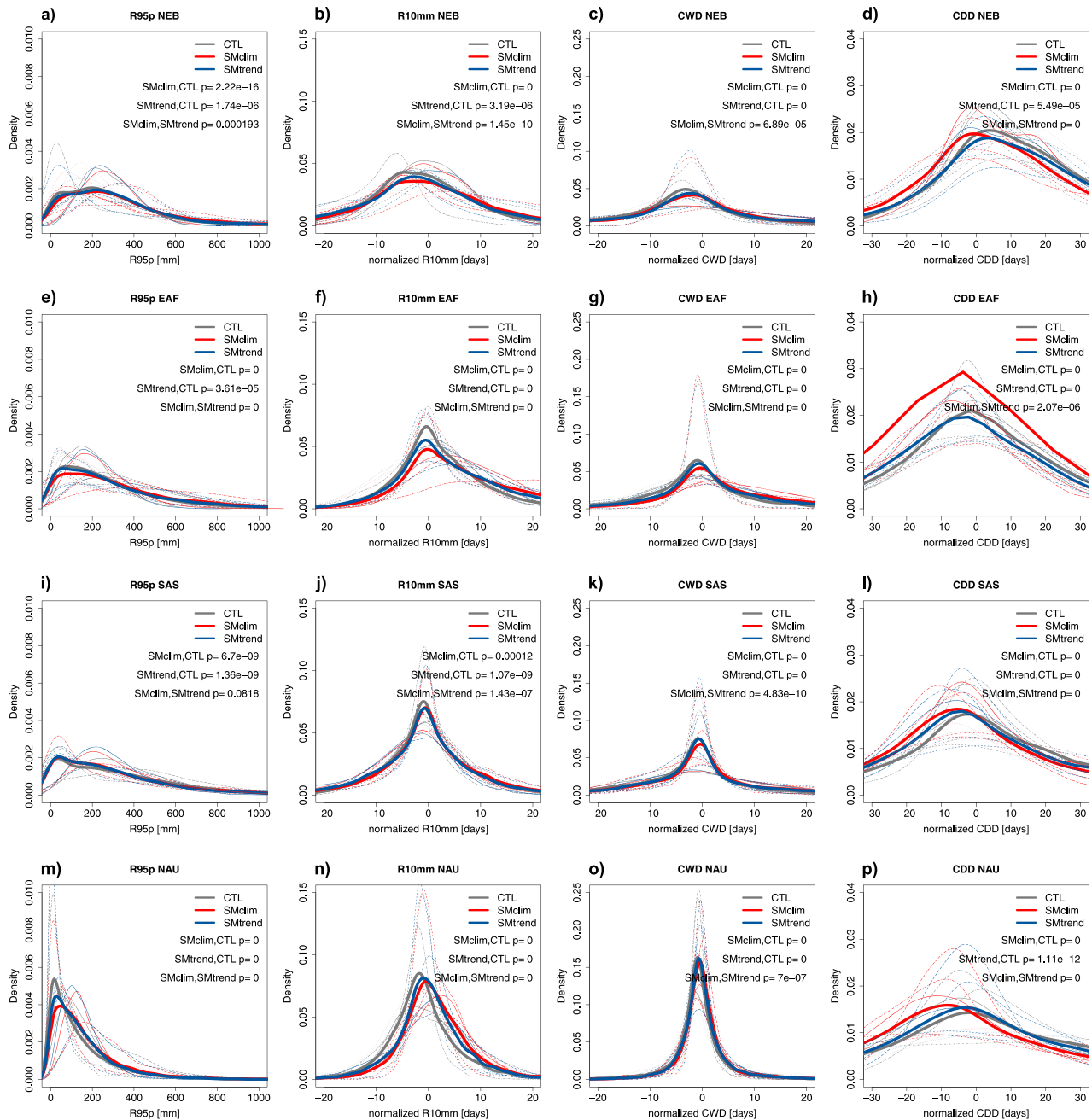
Figure 6. Spatially aggregated pdfs for precipitation indices in the second half of the 21st century (2056–2085). The thin lines indicate the individual models, the same line type for the same model, and the thick lines are the aggregated multimodel pdfs. R10mm, CDD, and CWD were normalized by removing the mean from each model's CTL. The regions are (a–d) North East Brazil (NEB), (e–h) East Africa (EAF), (i–l) South Asia (SAS), and (m–p) North Australia (NAU). The numbers indicate the p values of the Kolmogorov-Smirnov test comparing the pdfs from the different simulations.

moisture-precipitation feedback at daily timescales. Hence, the result of a positive soil moisture-precipitation feedback reported here has to be taken with caution.

4.2. Changes in Influence From Soil Moisture Variability

We find that the influence of soil moisture variability on frequency and duration of temperature extremes is projected to increase in the future. The difference between SMtrend and CTL is larger in the future period for TX90p and HWD (differences are small but statistically significant for TXx and not statistically significant for the precipitation extremes). *Seneviratne et al.* [2006] found a shift in regions where land-climate interactions play a role in the future using a similar experiment as our SMclim over Europe. We find that the regions where soil
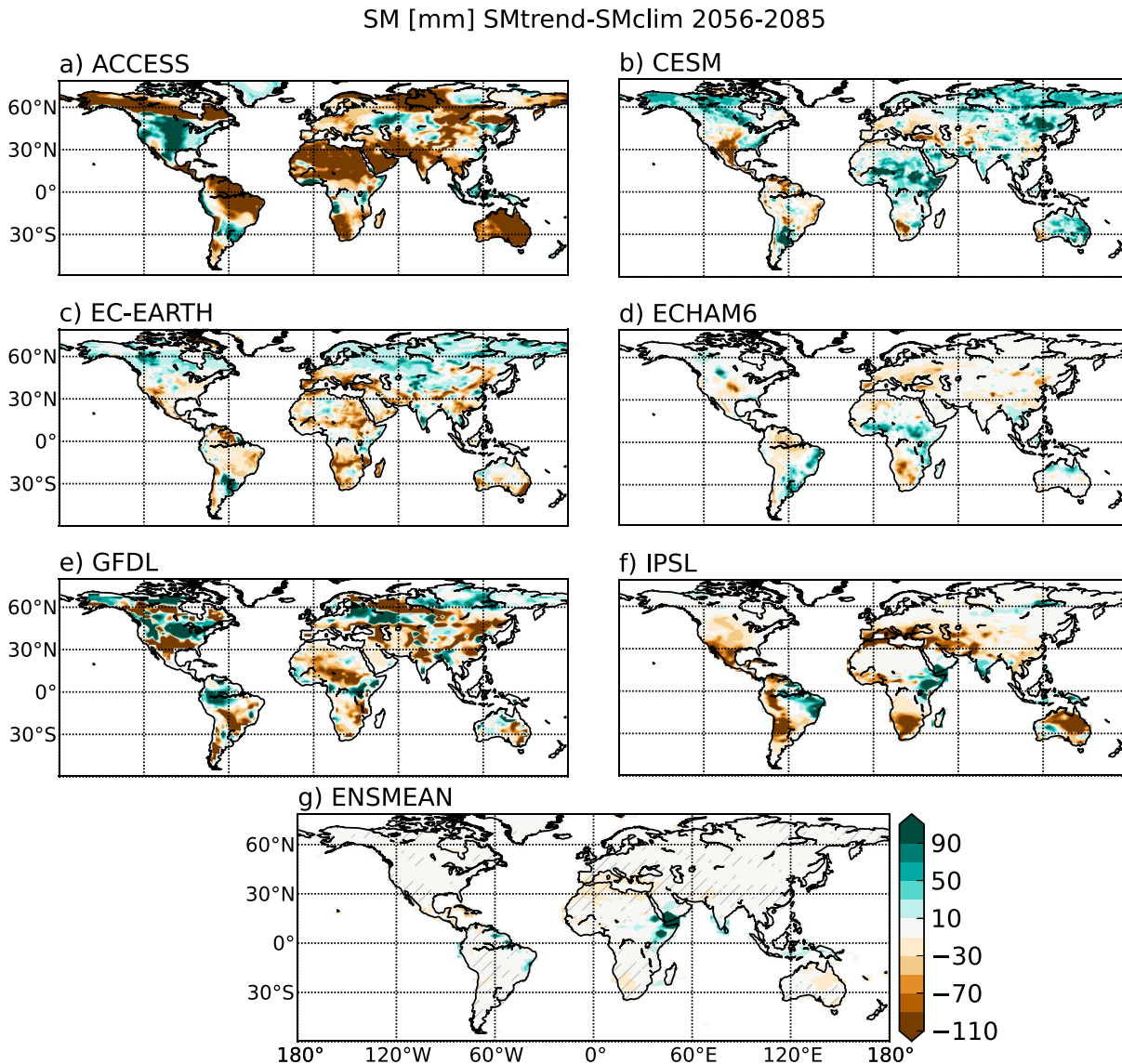
SM [%] SMtrend-SMclim 2056-2085
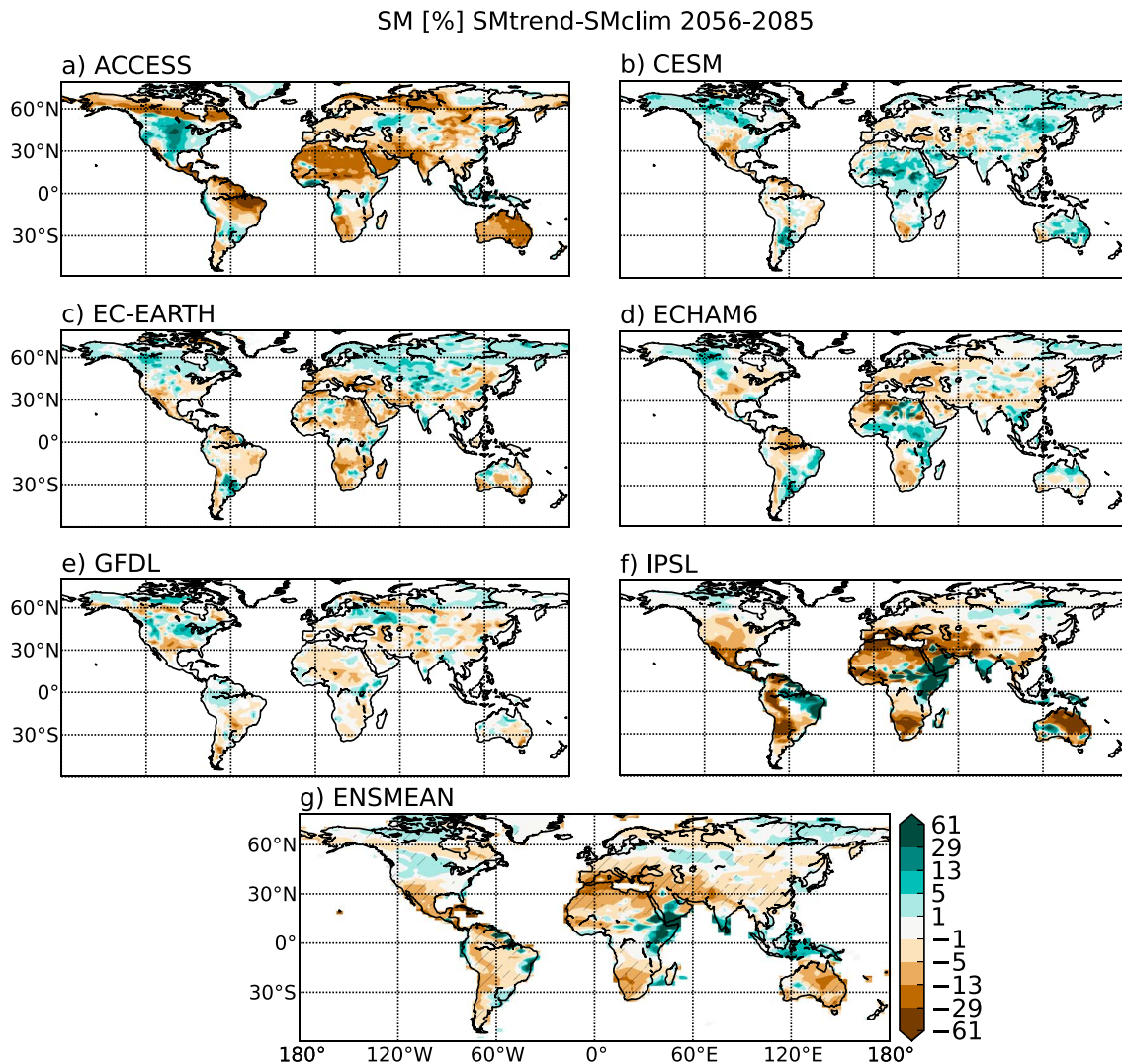
Figure 7. Soil moisture differences for SMtrend-SMclim, in percent relative to SMclim (1971–2000 climatology), in all GCMs in 2056–2085 and for the ensemble mean. Note that the scale is exponential. The hatching in the ensemble mean plot indicates where at least five out of six models agree in the sign of the difference.

moisture variability has an influence on TX90p and HWD remain similar in the future, but the influence itself becomes stronger. We do find a shift in region in South America for TX90p where our results suggest that the influence of soil moisture variability on TX90p is decreased in Amazonia, while it becomes more important in southern South America. The change in the effect of soil moisture variability may have implications for the contribution of soil moisture states to the predictability of extreme events.

4.3. Relationship to Soil Moisture Projections

S13 analyzed the first five GLACE-CMIP5 models in terms of their mean and the 95th percentile of temperature and precipitation and examined the impact of the soil moisture trend in the future and focusing on the Northern Hemisphere. They found increases in extreme daytime temperature of 2–2.5°C between SMclim (1A) and SMtrend (1B). For precipitation they found more heterogeneous results with mostly decreases in the Northern Hemisphere and Australia and mixed patterns in South America and Africa. We expand this analysis to three temperatures and four precipitation extreme indices that assess magnitude, frequency, and duration of extremes and place our analysis into context with the simulated soil moisture trends in the different models. Figure 7 shows the difference in 30 year mean soil moisture in the second half of this century for the experimental runs for each climate model. For each model, the difference is expressed in percent relative to the soil moisture level in SMclim (i.e., the 1971–2000 climatology) to normalize for different moisture

SM [mm] SMtrend-SMclim 2056-2085

Figure 8. Soil moisture differences for SMtrend-SMclim, in absolute mm water column, in all GCMs in 2056–2085 and for the ensemble mean. The hatching in the ensemble mean plot indicates where at least five out of six models agree in the sign of the difference.

holding capacities. First, note that the intermodel differences are large, with IPSL showing very large differences between end of century SMclim and SMtrend, while GFDL shows a lot less difference in soil moisture between SMclim and SMtrend. The absolute values of soil moisture differ between models (Figure 8), as do the relative changes towards the end of the 21st century (Figure 7). This is at least partially due to the fact that land surface models have structural differences, such as soil layering, total soil depths, and soil moisture capacity, and soil moisture is weakly constrained by observations in most regions of the world. Soil moisture is also influenced by many variables, such as precipitation, evapotranspiration, radiation, and clouds, and therefore reflects systematic biases in other model components. *Cheruy et al.* [2014] showed that deficiencies in the representation of clouds are involved both in a warm bias shared by most of the CMIP5 models over continental areas in summer and in the intensity of projected warming. Deep convective clouds are important for precipitation, which is the main driver of soil moisture availability; soil moisture in turn influences the boundary layer and the formation of clouds. Clouds also influence radiation, which then affects evapotranspiration and soil moisture. The combination of structural differences in the land surface schemes, climate biases, and differences in trends simulated by climate models makes soil moisture a variable difficult to simulate [*Kirtman et al.*, 2013]. Further, regional differences are very large. In some regions there is consistency between

the climate models; all models predict decreasing soil moisture levels in the Mediterranean, and all models except ACCESS predict decreasing soil moisture over Central North America. However, there is no intermodel agreement in the trend of soil moisture in some other regions such as Amazonia and the Sahel. Figures 1b, 1d, and 1f show a strong ensemble mean signal in regions where either the models agree on the sign of the soil moisture trend or at least one model has such a large trend that it dominates the ensemble. Clearly, using any multimodel ensemble or single model to examine land-atmosphere interactions into the future requires great care.

For the regions in Figures 5 and 8, CNA displays a drying trend in five out of six models, MED has a drying trend in all models, NAU has a drying trend in two out of six models, and SAF has a drying trend in all models, but this trend does not cover the whole region in EC-EARTH and CESM and is very small in GFDL. In all four regions, the ensemble mean projection is a drying trend. The large differences in the pdfs for TXx in NAU in SMtrend (thin blue lines) are related to the large differences among climate models regarding the long-term soil moisture changes in Australia. The individual models agree much better for TXx in MED, where they also agree on the projected drying trend. This helps explain the results by S13 who found pronounced increases in mean and extreme temperature over the Mediterranean region. However, differences between regions are also related to different background climates, climate variability, and importance of land-climate feedbacks [*Seneviratne et al.*, 2006; *Pitman et al.*, 2011; *Cheruy et al.*, 2014].

Our results have significant implications for the interpretation of simulated future temperature extremes. The results in Figure 5 highlight major differences on how individual models respond to the removal of interannual variability in soil moisture (SMclim) or its removal in combination with the simulated trend (SMtrend). Previous examination of how climate models simulate future changes in TXx and TX90p [*Sillmann et al.*, 2013; *Collins et al.*, 2013] points to changes in TXx of 5–7°C under RCP8.5. Our results for SMclim and SMtrend indicate that soil moisture variability and soil moisture trends are responsible for around 15% of these amounts (0.5–3.5°C) but over widespread regions of the continents. In other words, if soil moisture variability and/or soil moisture trends are not captured correctly in a model simulation, errors of up to 15% in TXx would result. Because TXx is an extreme value, errors of 15% are likely significant. Our problem, of course, is that Figure 5 shows very wide variations among models, something highlighted since *Koster et al.* [2006]. For TX90p, *Sillmann et al.* [2013] (their supporting information) suggest increases of 50–90% depending on the region, and *Collins et al.* [2013] suggest globally averaged increases by 2100 under RCP8.5 of around 55–65%. Our results suggest that soil moisture variability contributes up to 10%, and trends contribute up to 15–20% of the increases caused by changes in forcing prescribed in RCP8.5.

For precipitation the projected changes are already uncertain [*Kirtman et al.*, 2013; *Sillmann et al.*, 2013], which is reflected in the large differences between the models on how they project changes in soil moisture. The response of precipitation extremes to soil moisture is even more uncertain because the sign of the soil moisture-precipitation feedback is site and condition specific, and the ability of models to correctly resolve it remains to be established. We find a decrease in most wet precipitation extremes in SMtrend compared to SMclim in the future and an increase in the length of dry periods. *Sillmann et al.* [2013] report changes in R95p of up to 40–100% for RCP8.5, we find differences of 15–50% due to possible trends in soil moisture. Hence, soil moisture feedbacks might contribute up to 50% to the projected changes in extreme precipitation intensity by the end of the century. However, the projected changes of precipitation itself are more uncertain than those of temperature.

Differences in indices like TXx and TX90p of 15–20% due to the removal of soil moisture variability and trends would merely be an interesting modeling study were it not for the uncertainty on how climate models represent soil moisture now and in the future. *Kirtman et al.* [2013] note that future changes in soil moisture are very uncertain among models, a result illustrated by both their Figure 11.14 and our Figures 7 and 8. The uncertainty in soil moisture is influenced by the uncertainty in projections for the atmospheric forcing (i.e., precipitation and net radiation), flux partitioning at the surface, or a combination of both. It would be very interesting to know to which extent the differences in soil moisture are driven by different land model physics relative to climate forcing. Unfortunately this question is difficult to investigate with the current GLACE-CMIP5 model ensemble because of the differences in the atmospheric parts of the GCMs, and the feedbacks between land and atmosphere in these model runs. In short, there is poor agreement, particularly at regional scales, among models on how soil moisture is projected to change in the future and even on the sign of the soil moisture trend under RCP8.5, a result also highlighted in *Orlowsky and Seneviratne* [2013]. Our results show

that both soil moisture trends and variability affect TXx, TX90p, HWD, and possibly precipitation extremes. Therefore, they imply that it is necessary to resolve uncertainties in the simulation of soil moisture variability and soil moisture trends if the community wants to increase confidence on how temperature and precipitation extremes are expected to change on the regional level in the future.

5. Conclusions

We have shown that soil moisture variability has an important influence on the intensity, frequency, and duration of temperature extremes over land at the global scale. It is only where soil moisture variability is very small or in areas where energy, rather than soil moisture, limits evaporation (e.g., at high latitudes) that temperature extremes are not significantly influenced by soil moisture variability. Precipitation extremes are also influenced by soil moisture variability, but this impact is more heterogeneous. The largest impacts from soil moisture variability regard heavy precipitation in the tropics, and dry periods in the midlatitudes, in particular the Mediterranean region.

Long-term changes in soil moisture are also shown to exert a strong influence on projected temperature and precipitation extremes, even though the models included here show large uncertainties in the projection of long-term soil moisture trends. Overall, the most significant differences for SMtrend-SMclim occur where the models do agree on the existence of a soil moisture trend. Where the overall soil moisture projection is a drying trend, temperature extremes are projected to further increase in intensity, frequency, and duration. For precipitation extremes we find a decrease in heavy precipitation intensity and frequency, while dry periods become longer in areas where soil moisture is projected to decrease. In addition, we find that the influence of soil moisture variability on frequency and duration of temperature extremes is projected to increase in the future.

In conclusion, the accurate simulation of both soil moisture variability and long-term changes is necessary to correctly project future climate extremes. This is problematic because the models do not agree on these soil moisture features at the regional scale, perhaps with the important exceptions of the Mediterranean region as well as parts of South Africa and Central North America, where all models tend to predict a drying trend in the future (see also recent IPCC assessments: *Seneviratne et al.* [2012] and *Collins et al.* [2013]). We note that the general agreement of models in some regions does not necessarily mean it is correct. Obviously, soil moisture is largely dependent on precipitation, a variable for which the climate models also do not agree at the regional scales. This uncertainty is further increased for heavy precipitation extremes in the tropics that also depend on soil moisture variability. Soil moisture also depends on a wide range of land surface processes. Resolving the challenges highlighted here, and improving the confidence in regional projections of temperature and precipitation extremes, will require major advances in the modeling of land surface processes, precipitation, and clouds in the next generation of global climate models.

References

Alexander, L. V., et al. (2006), Global observed changes in daily climate extremes of temperature and precipitation, *J. Geophys. Res.*, *111*, D05109, doi:10.1029/2005JD006290.

Berg, A., et al. (2015), Interannual coupling between summertime surface temperature and precipitation over land: Processes and implications for climate change, *J. Clim.*, *28*, 1308–1328, doi:10.1175/JCLI-D-14-00324.1.

Berg, A. M., B. R. Lintner, K. L. Findell, P. Gentine, and S. Malyshev (2014), Impact of soil moisture-atmosphere interactions on surface temperature distribution, *J. Clim.*, *27*, 7976–7993, doi:10.1175/JCLI-D-13-00591.1.

Bi, D., et al. (2013), The ACCESS coupled model: Description, control climate and evaluation, *Aust. Meteorol. Oceanogr. J.*, *63*, 9–32.

Cheruy, F., J. L. Dufresne, F. Hourdin, and A. Ducharne (2014), Role of clouds and land-atmosphere coupling in midlatitude continental summer warm biases and climate change amplification in CMIP5 simulations, *Geophys. Res. Lett.*, *41*, 6493–6500, doi:10.1002/2014GL061145.

Collins, M., et al. (2013), Long-term climate change: Projections, commitments and irreversibility, in *Climate Change 2013: The Physical Science Basis. Contribution of Working Group I to the Fifth Assessment Report of the Intergovernmental Panel on Climate Change*, vol. 12, edited by T. F. Stocker et al., pp. 1029–1136, Cambridge Univ. Press, Cambridge, U. K., and New York.

Diro, G. T., L. Sushama, A. Martynov, D. I. Jeong, D. Verseghy, and K. Winger (2014), Land-atmosphere coupling over North America in CRCM5, *J. Geophys. Res. Atmos.*, *119*, 11,955–11,972, doi:10.1002/2014JD021677.

Donat, M. G., et al. (2013), Updated analyses of temperature and precipitation extreme indices since the beginning of the twentieth century: The HadEX2 dataset, *J. Geophys. Res. Atmos.*, *118*, 2098–2118, doi:10.1002/jgrd.50150.

Donat, M. G., A. D. King, J. T. Overpeck, L. V. Alexander, I. Durre, and D. J. Karoly (2015), Extraordinary heat during the 1930s US Dust Bowl and associated large-scale conditions, *Clim. Dyn.*,1–14, doi:10.1007/s00382-015-2590-5.

Douville, H. (2002), Influence of soil moisture on the Asian and African monsoons. Part II: Interannual variability, *J. Clim.*, *15*(7), 701–720, doi:10.1175/1520-0442(2002)015<0701:IOSMOT>2.0.CO;2.

Durre, I., J. M. Wallace, and D. P. Lettenmaier (2000), Dependence of extreme daily maximum temperatures on antecedent soil moisture in the contiguous United States during summer, *J. Clim.*, *13*(14), 2641–2651, doi:10.1175/1520-0442(2000)013<2641:DOEDMT>2.0.CO;2.

Easterling, D. R., G. A. Meehl, C. Parmesan, S. A. Changnon, T. R. Karl, and L. O. Mearns (2000), Climate extremes: Observations, modeling, and impacts, *Science*, *289*(5487), 2068–2074, doi:10.1126/science.289.5487.2068.

Ek, M. B., and A. A. M. Holtslag (2004), Influence of soil moisture on boundary layer cloud development, *J. Hydrometeorol.*, *5*(1), 86–99, doi:10.1175/1525-7541(2004)005<0086:IOSMOB>2.0.CO;2.

Eltahir, E., and R. L. Bras (1996), Precipitation recycling, *Rev. Geophys.*, *34*(3), 367–378.

Fischer, E. M., and R. Knutti (2014), Detection of spatially aggregated changes in temperature and precipitation extremes, *Geophys. Res. Lett.*, *41*, 547–554, doi:10.1002/2013GL058499.

Fischer, E. M., S. I. Seneviratne, D. Lüthi, and C. Schär (2007), Contribution of land-atmosphere coupling to recent European summer heat waves, *Geophys. Res. Lett.*, *34*, L06707, doi:10.1029/2006GL029068.

Fischer, E. M., U. Beyerle, and R. Knutti (2013), Robust spatially aggregated projections of climate extremes, *Nat. Clim. Change*, *3*(12), 1033–1038, doi:10.1038/nclimate2051.

Fischer, E. M., J. Sedláček, E. Hawkins, and R. Knutti (2014), Models agree on forced response pattern of precipitation and temperature extremes, *Geophys. Res. Lett.*, *41*, 8554–8562, doi:10.1002/2014GL062018.

Ford, T. W., and S. M. Quiring (2014), In situ soil moisture coupled with extreme temperatures: A study based on the Oklahoma Mesonet, *Geophys. Res. Lett.*, *41*, 4727–4734, doi:10.1002/2014GL060949.

Frei, C., R. Schöll, S. Fukutome, J. Schmidli, and P. L. Vidale (2006), Future change of precipitation extremes in Europe: Intercomparison of scenarios from regional climate models, *J. Geophys. Res.*, *111*, D06105, doi:10.1029/2005JD005965.

Frich, P., L. V. Alexander, P. M. Della-Marta, B. Gleason, M. Haylock, A. M. G. Klein Tank, and T. Peterson (2002), Observed coherent changes in climatic extremes during the second half of the twentieth century, *Clim. Res.*, *19*, 193–212.

Gates, W. L. (1992), AMIP: The atmospheric model intercomparison project, *Bull. Am. Meteorol. Soc.*, *73*(12), 1962–1970, doi:10.1175/1520-0477(1992)073<1962:ATAMIP>2.0.CO;2.

Goessling, H. F., and C. H. Reick (2011), What do moisture recycling estimates tell us? Exploring the extreme case of non-evaporating continents, *Hydrol. Earth Syst. Sci.*, *15*(10), 3217–3235, doi:10.5194/hess-15-3217-2011.

Guillod, B. P., B. Orlowsky, D. G. Miralles, A. J. Teuling, and S. I. Seneviratne (2015), Reconciling spatial and temporal soil moisture effects on afternoon rainfall, *Nat. Commun.*, *6*, 6443, doi:10.1038/ncomms7443.

Haarsma, R. J., F. Selten, B. V. Hurk, W. Hazeleger, and X. Wang (2009), Drier Mediterranean soils due to greenhouse warming bring easterly winds over summertime central Europe, *Geophys. Res. Lett.*, *36*, L04705, doi:10.1029/2008GL036617.

Hirsch, A. L., A. J. Pitman, S. I. Seneviratne, J. P. Evans, and V. Haverd (2014), Summertime maximum and minimum temperature coupling asymmetry over Australia determined using WRF, *Geophys. Res. Lett.*, *41*, 1546–1552, doi:10.1002/2013GL059055.

Hirschi, M., S. I. Seneviratne, V. Alexandrov, F. Boberg, C. Boroneant, O. B. Christensen, H. Formayer, B. Orlowsky, and P. Stepanek (2010), Observational evidence for soil-moisture impact on hot extremes in southeastern Europe, *Nat. Geosci.*, *4*(1), 17–21, doi:10.1038/ngeo1032.

Jaeger, E. B., and S. I. Seneviratne (2011), Impact of soil moisture-atmosphere coupling on European climate extremes and trends in a regional climate model, *Clim. Dyn.*, *36*(9–10), 1919–1939, doi:10.1007/s00382-010-0780-8.

Kirtman, B., et al. (2013), Near-term climate change: Projections and predictability, in *Climate Change 2013: The Physical Science Basis. Contribution of Working Group I to the Fifth Assessment Report of the Intergovernmental Panel on Climate Change*, edited by T. Stocker et al., pp. 953–1028, Cambridge Univ. Press, Cambridge, U. K., and New York.

Koster, R. D., et al. (2006), GLACE: The global land-atmosphere coupling experiment. Part I: Overview, *J. Hydrometeorol.*, *7*(4), 590–610, doi:10.1175/JHM510.1.

Koster, R. D., H. Wang, S. D. Schubert, M. J. Suarez, and S. Mahanama (2009), Drought-induced warming in the continental United States under different SST regimes, *J. Clim.*, *22*(20), 5385–5400, doi:10.1175/2009JCLI3075.1.

Kowalczyk, E. A., L. Stevens, R. M. Law, M. Dix, Y. P. Wang, I. N. Harman, K. Haynes, J. Srbinovsky, B. Pak, and T. Ziehn (2013), The land surface model component of ACCESS: Description and impact on the simulated surface climatology, *Aust. Meteorol. Oceanogr. J.*, *63*, 65–82.

Lorenz, R., E. L. Davin, D. M. Lawrence, R. Stöckli, and S. I. Seneviratne (2013), How important is vegetation phenology for European climate and heat waves?, *J. Clim.*, *26*(24), 10,077–10,100, doi:10.1175/JCLI-D-13-00040.1.

Lorenz, R., A. J. Pitman, M. G. Donat, A. L. Hirsch, J. Kala, E. A. Kowalczyk, R. M. Law, and J. Srbinovsky (2014), Representation of climate extreme indices in the ACCESS1.3b coupled atmosphere-land surface model, *Geosci. Model Dev.*, *7*(2), 545–567, doi:10.5194/gmd-7-545-2014.

Lorenz, R., A. J. Pitman, A. L. Hirsch, and J. Srbinovsky (2015), Intraseasonal versus interannual measures of land-atmosphere coupling strength in a global climate model: GLACE-1 versus GLACE-CMIP5 experiments in ACCESS1.3b, *J. Hydrometeorol.*, *16*, 2276–2295, doi:10.1175/JHM-D-14-0206.1.

May, W., A. Meier, M. Rummukainen, A. Berg, F. Chéruy, and S. Hagemann (2015), Contributions of soil moisture interactions to climate change in the tropics in the GLACE-CMIP5 experiment, *Clim. Dyn.*, *45*, 3275–3297, doi:10.1007/s00382-015-2538-9.

Meinshausen, M., et al. (2011), The RCP greenhouse gas concentrations and their extensions from 1765 to 2300, *Clim. Change*, *109*, 213–241, doi:10.1007/s10584-011-0156-z.

Miralles, D. G., M. J. van den Berg, A. J. Teuling, and R. A. M. de Jeu (2012), Soil moisture-temperature coupling: A multiscale observational analysis, *Geophys. Res. Lett.*, *39*, L21707, doi:10.1029/2012GL053703.

Mueller, B., and S. I. Seneviratne (2012), Hot days induced by precipitation deficits at the global scale, *Proc. Natl. Acad. Sci. U.S.A.*, *109*(31), 12,398–12,403, doi:10.1073/pnas.1204330109.

Orlowsky, B., and S. I. Seneviratne (2011), Global changes in extreme events: Regional and seasonal dimension, *Clim. Change*, *110*(3–4), 669–696, doi:10.1007/s10584-011-0122-9.

Orlowsky, B., and S. I. Seneviratne (2013), Elusive drought: Uncertainty in observed trends and short-and long-term CMIP5 projections, *Hydrol. Earth Syst. Sci.*, *17*(5), 1765–1781, doi:10.5194/hess-17-1765-2013.

Perkins, S. E., and L. V. Alexander (2013), On the measurement of heat waves, *J. Clim.*, *26*(13), 4500–4517, doi:10.1175/JCLI-D-12-00383.1.

Perkins, S. E., L. V. Alexander, and J. R. Nairn (2012), Increasing frequency, intensity and duration of observed global heatwaves and warm spells, *Geophys. Res. Lett.*, *39*, L20714, doi:10.1029/2012GL053361.

Pitman, A. J., F. B. Avila, G. Abramowitz, Y. P. Wang, S. J. Phipps, and N. de Noblet-Ducoudré (2011), Importance of background climate in determining impact of land-cover change on regional climate, *Nat. Clim. Change*, *1*(9), 472–475, doi:10.1038/nclimate1294.

Pitman, A. J., et al. (2012), Effects of land cover change on temperature and rainfall extremes in multi-model ensemble simulations, *Earth Syst. Dyn.*, *3*(2), 213–231, doi:10.5194/esd-3-213-2012.

Quesada, B., R. Vautard, P. Yiou, M. Hirschi, and S. I. Seneviratne (2012), Asymmetric European summer heat predictability from wet and dry southern winters and springs, *Nat. Clim. Change*, *2*(10), 736–741, doi:10.1038/nclimate1536.

Schär, C., D. Lüthi, U. Beyerle, and E. Heise (1999), The soil-precipitation feedback: A process study with a regional climate model, *J. Clim.*, *12*, 722–741, doi:10.1175/1520-0442(1999)012<0722:TSPFAP>2.0.CO;2.

Seneviratne, S. I., D. Lüthi, M. Litschi, and C. Schär (2006), Land-atmosphere coupling and climate change in Europe, *Nature*, *443*(7108), 205–209, doi:10.1038/nature05095.

Seneviratne, S. I., T. Corti, E. L. Davin, M. Hirschi, E. B. Jaeger, I. Lehner, B. Orlowsky, and A. J. Teuling (2010), Investigating soil moisture-climate interactions in a changing climate: A review, *Earth Sci. Rev.*, *99*(3–4), 125–161, doi:10.1016/j.earscirev.2010.02.004.

Seneviratne, S. I., et al. (2012), Changes in climate extremes and their impacts on the natural physical environment, in *Managing the Risks of Extreme Events and Disasters to Advance Climate Change Adaptation*, edited by C. B. Field et al., pp. 109–230, Cambridge Univ. Press, Cambridge, U. K., and New York.

Seneviratne, S. I., et al. (2013), Impact of soil moisture-climate feedbacks on CMIP5 projections: First results from the GLACE-CMIP5 experiment, *Geophys. Res. Lett.*, *40*, 5212–5217, doi:10.1002/grl.50956.

Sillmann, J., V. V. Kharin, F. W. Zwiers, X. Zhang, and D. Bronaugh (2013), Climate extremes indices in the CMIP5 multimodel ensemble: Part 2. Future climate projections, *J. Geophys. Res. Atmos.*, *118*, 2473–2493, doi:10.1002/jgrd.50188.

Sörensson, A. A., and C. G. Menéndez (2011), Summer soil-precipitation coupling in South America, *Tellus, Ser. A*, *63*(1), 56–68, doi:10.1111/j.1600-0870.2010.00468.x.

Taylor, C. M., A. Gounou, F. Guichard, P. P. Harris, R. J. Ellis, F. Couvreux, and M. De Kauwe (2011), Frequency of Sahelian storm initiation enhanced over mesoscale soil-moisture patterns, *Nat. Geosci.*, *4*(7), 430–433, doi:10.1038/ngeo1173.

Taylor, C. M., C. E. Birch, D. J. Parker, N. Dixon, F. Guichard, G. Nikulin, and G. M. S. Lister (2013), Modeling soil moisture-precipitation feedback in the Sahel: Importance of spatial scale versus convective parameterization, *Geophys. Res. Lett.*, *40*, 6213–6218, doi:10.1002/2013GL058511.

Vautard, R., P. Yiou, F. D'Andrea, N. de Noblet, N. Viovy, C. Cassou, J. Polcher, P. Ciais, M. Kageyama, and Y. Fan (2007), Summertime European heat and drought waves induced by wintertime Mediterranean rainfall deficit, *Geophys. Res. Lett.*, *34*, L07711, doi:10.1029/2006GL028001.

Williams, C. J. R., R. P. Allan, and D. R. Kniveton (2012), Diagnosing atmosphere-land feedbacks in CMIP5 climate models, *Environ. Res. Lett.*, *7*(4), 044003, doi:10.1088/1748-9326/7/4/044003.

Yin, D., M. L. Roderick, G. Leech, F. Sun, and Y. Huang (2014), The contribution of reduction in evaporative cooling to higher surface air temperatures during drought, *Geophys. Res. Lett.*, *41*, 7891–7897, doi:10.1002/2014GL062039.

Zampieri, M., F. D'Andrea, R. Vautard, P. Ciais, N. de Noblet-Ducoudré, and P. Yiou (2009), Hot European summers and the role of soil moisture in the propagation of Mediterranean Drought, *J. Clim.*, *22*(18), 4747–4758, doi:10.1175/2009JCLI2568.1.